https://doi.org/10.31925/farmacia.2018.4.19

ORIGINAL ARTICLE

DNA INTERCALATING ABILITY OF FOUR ACRIDINE-*N*-OXYDES DERIVATIVES INVESTIGATED BY SPECTRAL AND ELECTROCHEMICAL TECHNIQUES

MIHAELA TERTIŞ [1], MONICA BUCŞA [2], GRAŢIELA MESEŞAN [1], ADRIAN PÎRNĂU [3], CĂLIN G. FLOARE [3], ROBERT SĂNDULESCU [1], CECILIA CRISTEA [1]*

[1]*Analytical Chemistry Department, Faculty of Pharmacy, "Iuliu Haţieganu" University of Medicine and Pharmacy, 4 Louis Pasteur Street, 400349, Cluj-Napoca, Romania*
[2]*"Raluca Ripan" Institute for Research in Chemistry, "Babeş-Bolyai" University, 30 Fântânele Street, 400294, Cluj-Napoca, Romania*
[3]*National Institute for Research and Development of Isotopic and Molecular Technologies, 67-103 Donat Street, 400293, Cluj-Napoca, Romania*

**corresponding author: ccristea@umfcluj.ro*

Manuscript received: January 2018

Abstract

Acridines belong to one of the most frequently studied class of compounds due to their numerous physico-chemical properties and their biological action. Thus, the use of acridines as antitumor, antibacterial, antiviral, antimalarial and anti-nociceptive agents is known. Antitumour action is due to their ability to interfere with the structure of deoxyribonucleic acid (DNA), thereby disrupting its normal functioning. Electrochemical and spectral behaviour of the four compounds were investigated showing that only one *N*-oxyde acridine has the ability to intercalate into the single strand DNA (ssDNA). The binding constant was computed using ^{1}H-NMR.

Rezumat

Acridinele se numără printre cei mai frecvent studiaţi compuşi datorită numeroaselor proprietăţi fizico-chimice şi acţiunii lor biologice. Astfel, este cunoscută utilizarea acridinelor ca agenţi antitumorali, antibacterieni, antivirali, antimalarieni şi anti-nociceptivi. Acţiunea antitumorală se datorează capacităţii lor de a interfera cu structura acidului dezoxiribonucleic (ADN), perturbând astfel funcţionarea sa normală. Comportamentul electrochimic şi cel spectral a patru derivaţi de *N*-oxid acridină au fost investigate, arătând capacitatea de intercalare în structura ADN-ului doar a derivatului 9-metoxi-*N*-acridină. Calculul constantei de legare între acest derivat de acridină şi ADN a fost realizat cu ajutorul ^{1}H-RMN.

Keywords: acridine-*N*-oxydes, electrochemistry, carbon-based electrodes, UV-Vis spectra, ^{1}H-NMR spectra

Introduction

Organic intercalating agents are a class of poly-aromatic compounds that are extensively studied because of the numerous properties they possess such as antitumor, antibacterial (anti-TB), antiviral (anti-HIV), antiprotozoal, antimalarial and anti-nociceptive. These compounds can be inserted or intercalated between two adjacent base pairs, inhibiting *in vivo* synthesis of nucleic acid.

Antitumour action is due to their ability to intercalate into the DNA structure and to inhibit cyclin-dependent topoisomerase, telomerase and cyclin-dependent protein kinases [3, 9]. Generally, acridines can interact with DNA either through the pairs of nitrogen bases or through one of the two DNA strands, blocking replication, transcription, or repair of the DNA. The acridine compounds also have the ability to inhibit topoisomerase I and II, these actions leading to cell death.

Intercalation of acridines between the pairs of nitrogenous bases formed by the two strands of DNA is accomplished by non-covalent interactions (ionic, hydrophobic, hydrogen bonds and van der Waals). The insertion of an intercalation agent between the adjacent base pairs leads to substantial changes in the DNA structure, with deep alterations of the secondary nucleotide structure.

Thus, the presence of an intercalation agent between the two pairs of nitrogenous bases prevents the access of another intercalation agent to or adjacent to the binding site in question. In this way, each second binding site on the length of the DNA strand remains unoccupied [13].

DNA and RNA based biosensors, also called geno-sensors, use the unique properties of these receptors. Genosensors are of major interest because of their applicability in detecting an unlimited number of compounds from small ions to macromolecular compounds, such as polymers or proteins [14].

In the last decades, the property of intercalating compounds has been focused on the interfering capabilities with the structure of DNA. The use of these compounds to study DNA structure has also been addressed based on the interactions between DNA and drug and between DNA and protein, respectively [12, 13].

Acridines interact with double stranded DNA (dsDNA) by including pairs of adjacent nitrogen bases, but also by π-type interactions with certain pairs of nucleic bases. The formation of complex combinations with DNA by intercalation usually causes the occurrence of hypochromic or bathochromic effect in the molecular absorption spectra of the compounds involved in complexation. These phenomena are due to the occurrence of strong interactions between the aromatic chromophore and the pairs of nitrogenous bases in the DNA structure where the intercalation occurs [2, 11]. Other acridines derivatives like methylene blue or proflavine were successfully used as intercalating agents in DNA structure and applied in the labelling of several genosensors and aptasensors [4, 6, 8, 10].

The voltamperometric determinations were performed in order to determine the optimal conditions for the reduction and electrochemical oxidation processes of the acridine derivatives as well as the dependence of these processes on different factors: electrode material, type of electrolyte and its nature, pH and concentration of the reactant in the electrolyte solution.

The bathochromic and hypochromic displacement of the signals from the molecular absorption spectra recorded after intercalation of some chromophores in DNA strands was also cited by other authors [7, 15]. Thus, to prove the possibility of intercalating in the dopamine specific DNA strand of the investigated acridines, spectroscopic titrations of these compounds with the aptamers were performed.

The spectral and electrochemical study of four acridines, namely: acridine-*N*-oxide **(A1)** and its derivatives functionalized to the 9-position with the cyan group (9-cyan-acridine-*N*-oxide: **A2**), with carboxyl group (9-carboxy-acridine-*N*-oxide: **A3**) and with methoxy group (9-methoxy-acridine-*N*-oxide: **A4**) are presented, having the main idea of testing their ability to be used as intercalating agents for the design of novel aptasensors. The association constant was computed after spectral studies by using ^{1}H- NMR.

Materials and Methods

Reagents

The four acridines were synthesised and completely characterised as described in a previous paper [1].

The DNA sequence used has the following succession of 76 nitrogen bases: 5' GTCTCTGTGTGCGCCA GAGAACACTGGGGCAGATATGGGCCAGCAC AGAATGAGGCCTTTTTTTTTTTTTT 3', and 3' terminus functionalized with amino or thiol, depending on the practical necessity. This DNA sequence was synthesized for dopamine recognition and was purchased from Alpha DNA (Montreal, Canada). Potassium ferrocyanide ($K_4[Fe(CN)_6]$) and potassium ferricyanide ($K_3[Fe(CN)_6]$) were purchased from Sigma Aldrich, USA. Disodium hydrogen phosphate, sodium dihydrogen phosphate, TRIS-Cl, EtOH, KCl, NaOH, NaCl, HCl, H_2SO_4, $MgCl_2$, acetic acid sodium acetate, citric acid, sodium citrate and other reagents and solvents were purchased from Merck. All the reagents were of analytical grade and used as received without purification. The aqueous solutions including buffer solutions were prepared daily using MilliQ-ultrapure, deionized water.

The phosphate buffer stock solutions were prepared from 0.2 mol/L NaH_2PO_4 and 0.2 mol/L Na_2HPO_4 in ultrapure, demineralised water, diluted to 0.02 mol/L daily, and after filtration through Phenetex micro-filters were combined to obtain a pH = 7.4 solution. The 0.2 mol/L acetate buffer (pH = 4.5) was obtained by mixing 0.2 mol/L acetic acid and 0.1 mol/L sodium acetate solutions to the desired pH. The 0.002 mol/L citrate buffer was obtained from 0.1 mol/L citric acid stock solutions and 0.1 mol/L sodium citrate prepared in ultra-pure water for which the pH was adjusted to 6.5 with 2 mol/L NaOH solution. There were also used: 0.1 mol/L H_2SO_4 (pH = 2), 0.1 mol/L carbonate buffer (pH = 10.3). The pH adjustment was made with ChemCadet pH meter and all measurements were performed at room temperature (20 - 25ºC).

Equipment

To determine the electrochemical behaviour of the studied acridine derivatives: acridine-*N*-oxide (**A1**), 9-cyano-acridine-*N*-oxide (**A2**), 9-carboxyl acridine-*N*-oxide (**A3**) and 9-methoxy-acridine-*N*-oxide (**A4**), cyclic voltammetry (CV) and differential pulse voltammetry (DPV) experiments were performed with glassy carbon electrodes (GCE), gold electrodes, as well as carbon or gold screen printed electrodes (SPEs). The assays were performed in various buffer solutions such as 0.1 mol/L H_2SO_4 (pH = 2), 0.2 mol/L acetate buffer (pH = 4.5), 0.002 M citrate buffer (pH = 6.5), 0.1 mol/L TRIS buffer (pH = 7.2), 0.02 mol/L phosphate buffer saline (PBS) (pH = 7.4) and 0.1 mol/L carbon buffer (pH = 10.3). Before each determination, solutions were purged with nitrogen for 15 minutes to remove dissolved oxygen.

All electrochemical measurements were performed using an AutoLab PGSTAT 30 potentiostat/galvanostat (Ecochemie, The Netherlands) with GPES software and an AutoLab PGSTAT 100 potentiostat/galvanostat (Ecochemie, The Netherlands) with NOVA soft-ware 1.10.4.

Electrochemical determinations were performed in a three-electrode cell. The electrodes used in studies were purchased from BAS Inc. (West Lafayette, USA). The reference electrode was the Ag/AgCl

saturated electrode (3 mol/L KCl), and in the case of the auxiliary electrode a platinum electrode (spiral wire) was used. As working electrode, several electrode materials were used: glassy carbon (d = 3 mm) and gold (d = 2 mm). SPEs from DropSens (Spain) based on graphite (type 110) and gold (type 250) were also used. The electrochemical cell, in this case, printed on ceramic substrate, consists of a working electrode of graphite or gold, a graphite counter electrode and the silver reference pseudo-reference electrode.

All ^{1}H-NMR measurements were carried out with a Bruker AVANCE III spectrometer operating at 500.13 MHz for protons and equipped with a broad-band observation probe.

The NMR spectra were recorded in buffered D_2O/DMSO-d_6 solutions (1:2 ratio) at 298 ± 0.1 K and all chemical shifts were measured relative to TMS.

Preparation of acridine-N-oxydes stock solutions

The stock solutions of the four acridine-*N*-oxide compounds were prepared by dissolving the amounts corresponding to the concentration of 0.1 mol/L in 1 mL ethanol (for **A1, A2** and **A4**), respectively methanol for (**A3**), because these compounds exhibit very low aqueous solubility. These solutions were kept in dark and at 4°C, conditions in which they maintain their stability over a long period of time.

Spectral determinations

Spectrophotometric determinations were performed using a Specord250 PLUS (Analytical Jena, Germany) spectrophotometer equipped with WinAspect software. Determinations were made with acridine solutions in both the UV and visible fields. To determine the nature of the interactions between the acridine derivatives and the considered DNA sequence, stock solutions of 10^{-12} mol/L acridines, 10^{-6} mol/L aptamer and mixtures of 10^{-4} mol/L acridines and constant or variable concentrations of aptamer were used. UV-Vis spectra were recorded in 10 mmol/L TRIS-HCl buffer solution (pH = 7.2) and using quartz cuvettes with 1 cm optical path length at 25°C.

^{1}H-NMR experiment and spectral studies

For each ^{1}H-NMR experiment, between 32 and 256 transients were collected into 65 K data points over a 5000 Hz spectral window, using a 3 s relaxation delay. The 2D ^{1}H-^{1}H COSY NMR spectrum was acquired using 8 scans with a Bruker standard program (Pulse Program Cosygf45). Each spectrum consisted of a matrix of 1024/512 data points covering a spectral width of 2000 Hz.

Results and Discussion

The acridine-*N*-oxides and their derivatives are yellow compounds, have high melting points (greater than 169°C), are poorly soluble in non-polar solvents and have a more irritating effect on the skin and mucous membranes than the corresponding acridines. However, they are less toxic to the human body compared to the compounds they derive. They are generally soluble in alcohols (having green fluorescence in ethanol) in chloroform or *n*-hexane.

Spectral behaviour in the UV-Vis field of acridine derivatives

The formation of complex combinations with DNA by intercalation usually causes the occurrence of hypochromic or bathochromic shifts in the molecular absorption spectra of the compounds involved in complexation. These phenomena are due to the occurrence of strong interactions between the aromatic chromophore and the pairs of nitrogenous bases in the DNA structure where the intercalation occurs [2, 11].

In the case of the first three acridines spectra it can be observed the presence of absorption bands in the wavelength range from 340 to 460 nm (Figure 1), these bands being typical of the transitions processes that occur between the energetic levels of the acridine ring [17].

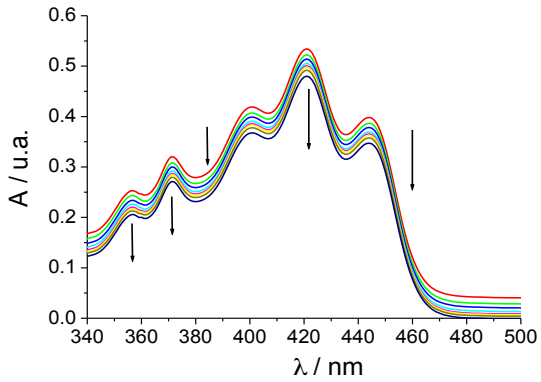

Figure 1.

Absorption spectra recorded in the UV-Vis range for a 0.1 mmol/L **A3** (red upper curve) solution in 0.1 mol/L TRIS buffer (pH = 7.4, 25°C) and increasing concentrations of apt-DA (from 50 nmol/L to 1.25 μmol/L). The molar ratios between **A3** and aptamer are as follows (from peak to base): 2000, 1000, 666, 66, 500, 200, 80

It was noticed that the presence of different substituent on the acridine-*N*-oxide nucleus (**A1**) determines the displacements of the positions where the acridinic chromophore signals occur both for **A2** and **A3**. For each compound, after adding the aptamer in the solution, no movement of the bands at other wavelengths is observed, but only a decrease in their intensity with the increase of the aptamer concentration, thus a hypochromic displacement of the signals was registered. Thus, for the **A1** derivative the hypochromic displacement of the five signals is in the range of 2.63% to 3.71% for the **A2** derivative, the hypochromic displacement of the five signals is in the range of 4.69% to 13.43%, and for derivative **A3**, the hypochromic displacement of the five signals

ranges from 9.94% to 19.92%. The results obtained for **A1, A2** and **A3** derivatives show that these three compounds do not form intercalation complexes with the dopamine-specific DNA sequence, but their complexes are governed by other types of interactions (adsorption, van der Waals bond formation, hydrogen bonds, etc.). Only the data obtained for **A3** are presented for exemplification.

The nature of the interactions between the **A4** derivative and the dopamine-specific DNA sequence have also been studied. In Figure 2, the changes occurring in the absorption spectra recorded during the titration of the **0**.1 mmol/L **A4** solution with increasing concentrations of aptamer (from 0 to 1.25 μmol/L) are observed. In the spectrum recorded for the **A4** solution, the presence of the five absorption bands in the wavelength range of 340 to 460 nm is observed, as in the case of the three compounds shown above.

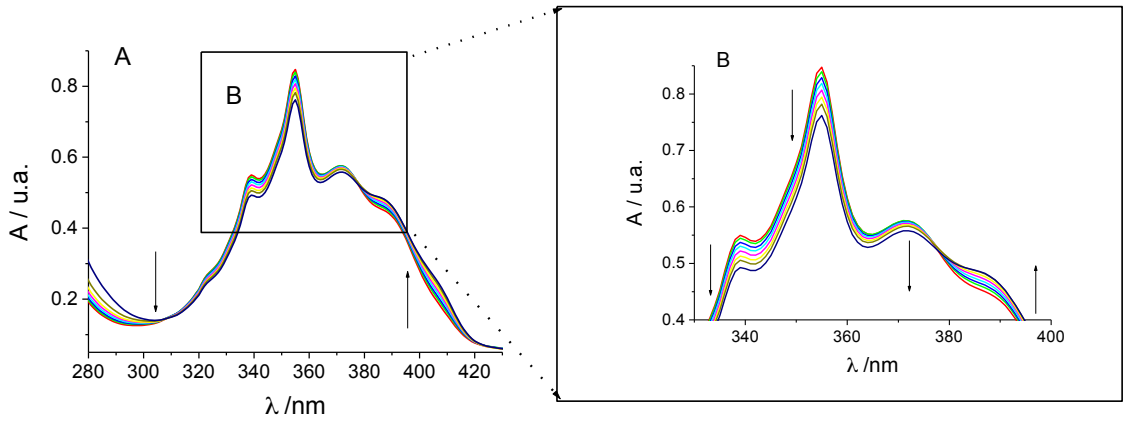

Figure 2.

(A) The absorption spectra recorded in the UV-Vis range for 0.1 mmol/L **A4** solution (red) compared to those recorded for mixtures of **A4** with increasing concentrations of apt-DA (from 50 nmol/L to 1.25 μmol/L); solution prepared in 0.1 mol/L TRIS buffer (pH = 7.4). The molar ratios between **A4** and aptamer are from peak to base: 2000, 1000, 666, 66, 500, 200, 80; (B) Details of the UV-Vis absorption spectra revealing the isosbestic point

It is noted that after the addition of aptamer in the solution, all characteristic bands move at higher wavelengths, with Δλ between 1.08 and 1.72 nm (bathochromic displacement), together with an intensity decrease of these bands with the increase of the aptamer concentration (hypochromic displacement of signals), ranging from 5.77% to 11.81%. Also, a partial loss of the fine structure of the absorption bands is observed with the increase of the aptamer concentration and the appearance of an isosbestic point at 380 nm (Figure 2B). This behaviour proves that the nature of interactions between the **A4** and the DNA sequence is the intercalation of the chromophore between the nitrate bases of the non-denatured aptamer structure.

For the **A4**, the ligand that has previously been shown to have the ability to intercalate in the DNA strand, the intercalation time has also been optimized. Thus, a solution was prepared containing both 0.1 mmol/L **A4** and 1 μmol/L dopamine-specific DNA sequence (apt-DA) prepared in 0.1 mol/L TRIS buffer (pH = 7.4, 25°C). This solution was recorded for different values of the contact time, and the results obtained are shown in Figure 2A.

In the near-field UV range, at wavelengths ranging from 240 to 260 nm, an absorption band is observed, the intensity of which decreases as the contact time increases from 3.51 at 2.44 units of absorbance, at the same time as the hyposochromic shift (to smaller wavelengths) from 254.13 nm initially to 252.44 nm after 12 hours (data not presented). Also, at wavelengths ranging from 320 to 420 nm, specific acridinium chromophore signals are observed, whose position and intensity vary differently with increasing the contact time (Figure 2A and 2B).

It is worth to mention that the first three characteristic bands in the spectrum move at higher wavelengths, with Δλ between 1.47 and 4.00 nm (bathochromic displacement), together with a decrease in the intensity of these bands with the increase of the contact time with aptamer (hypochromic shift of signals), ranging from 60.91% to 70.36%. The absorption band appearing at wavelength of 372.24 nm does not change its position and does not change its intensity, while the band appearing at 387.51 nm moves (bathochromic shift) with 0.83 nm and records a hyperchromic displacement of 78.85%. A new absorption band appears at a wavelength of 399.01 nm, which displaces bathochromic with 5.74 nm and records a hyperchromic with 186.52% with the increase of contact time. These data proved that the A4 derivative is the compound that associates with the aptamer by intercalation between the nitrate bases of the non denaturated DNA sequence.

Electrochemical behaviour of acridines derivatives

From the analysis of the CVs of acridine derivatives obtained with different electrode materials (glassy carbon, Au and graphite) it is observed that the presence of a different functional groups on the acridine ring determines the significant change in terms of number, position and intensity of the recorded signals, both in the field of oxidation and reduction potential.

CVs of the 10^{-4} mol/L solutions of the four acridine derivatives in 0.02 mol/L phosphate saline (PBS) (pH = 7.4) were obtained on GCE, gold electrodes as well as for graphite and gold SPE. The potential range was from -1.2 V to 1.0 V for the initial scan direction, then back to -1.2 V for return. Five cycles were performed (data not shown), the results obtained with respect to the position and intensity of the recorded oxidation and electrochemical reduction peaks are comparatively presented in Table I. It is worth to notice that all the acridines taken in the study showed a little oxidation peak, which is best observed on carbon-based electrodes. On Au-based electrodes, the oxidation potential is displaced in the anodic direction and the peak current intensity is significantly lower than that obtained on carbon, which recommends carbon-based materials for further experimental determinations of acridines by CV. Thus, potential oxidation at 0.27 V *vs*. Ag/AgCl in the case of GCE and 0.93 V *vs*. Ag/AgCl in the case of gold-based SPEs is observed for **A1**. For graphite SPE, the oxidation peak of **A1** occurs at 0.85 V *vs*. Ag/AgCl, the highest peak intensity being 34.01 μA (Table I). For **A2** and **A3**, under the same experimental conditions, glassy carbon was found to be the material that determines the highest intensity of the oxidation peak (Table I). For **A4**, the most marked oxidation signal also appears on carbon at 0.60 V *vs*. Ag/AgCl, (Table I).

When scanning the potential domain in the negative direction, on graphite electrode materials, a reduction peak was obtained between -0.69 V and -0.82 V *vs*. Ag/AgCl. There are two reduction peaks obtained on gold electrodes. It is known that Au-based electrodes have a greater affinity for higher and complex molecules presenting heteroatoms, adsorption phenomena being reported [16, 18].

Table I

Oxidation/reduction currents for **A1, A2, A3, A4** derivatives at different electrodes

Compound	Electrode material	Oxidation		Reduction	
		E_{ox} (V *vs*. Ag/AgCl)	$I_{max,ox}$ (μA)	E_{red} (V *vs*. Ag/AgCl)	$I_{max,red}$ (μA)
A1	GCE	0.27	5.83	-0.75	-24.52
	SPE-graphite	0.85	34.01	-	-
	Au	0.24	1.27	0.39	- 0.39
		0.59	1.79	-0.44	-10.07
	SPE-Au	0.13	3.13	0.36	- 2.56
		0.93	14.77	-0.25	- 1.93
				-0.69	-11.03
A2	GCE	0.25	6.40	-0.82	-45.13
	SPE-graphite	0.22	0.86	-	-
	Au	0.72	4.61	-0.38	-14.22
	SPE-Au	0.70	4.33	0.35	-10.21
		0.09	1.14	-0.55	-13.13
A3	GCE	0.42	5.02	-0.69	-12.04
	SPE-graphite	0.54	0.61	-	-
	Au	0.39	1.48	0.47	-0.18
		0.58	1.33	0.25	-0.33
		0.92	1.98	-0.39	-9.51
	SPE-Au	0.47	1.84	-	-
A4	GCE	0.60	7.47	-0.77	-20.60
	SPE-graphite	0.72	3.62	-	-
	Au	0.40	0.61	-0.51	-10.35
	SPE-Au	0.51	2.05	0.09	-1.08
		0.75	4.10		

For further studies glassy carbon was chosen as working electrode for the four acridines.

Influence of the supporting electrolyte. For the study of the supporting electrolyte influence on the electrochemical behaviour, CV measurements of the four acridine derivatives solutions in different electrolytic media (such as H_2SO_4, acetate buffer, citrate buffer, saline phosphate buffer, TRIS buffer and carbonate buffer) were made on GCE. The results obtained are shown in Figure 3 and comparative data in Table II.

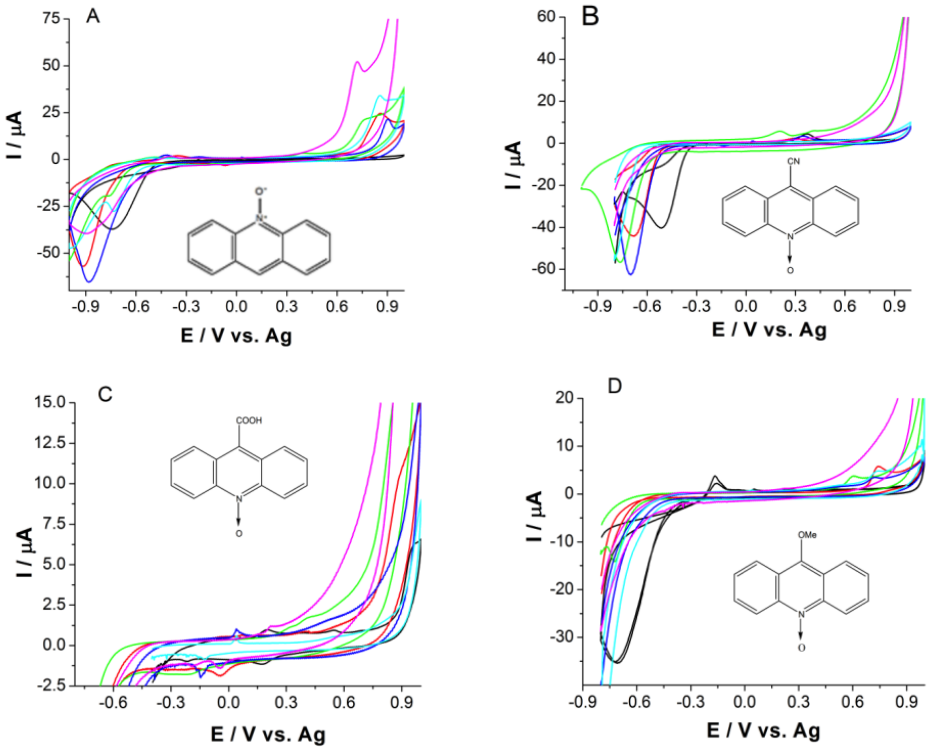

Figure 3.

CVs of 0.1 mmol/L acridines recorded at GCE: (A) **A1**; (B) **A2**; (C) **A3** and (D) **A4** solutions prepared in: H_2SO_4 mol/L (pH = 2; black); acetate buffer 0.1 mol/L (pH = 4.5; red); 0.002 mol/L citrate buffer (pH = 6.5; green); TRIS buffer 0.1 mol/L (pH = 7.2; blue); PBS 0.02 mol/L (pH = 7.4; light blue); 0.1 mol/L carbonate buffer (pH = 10.3; pink)

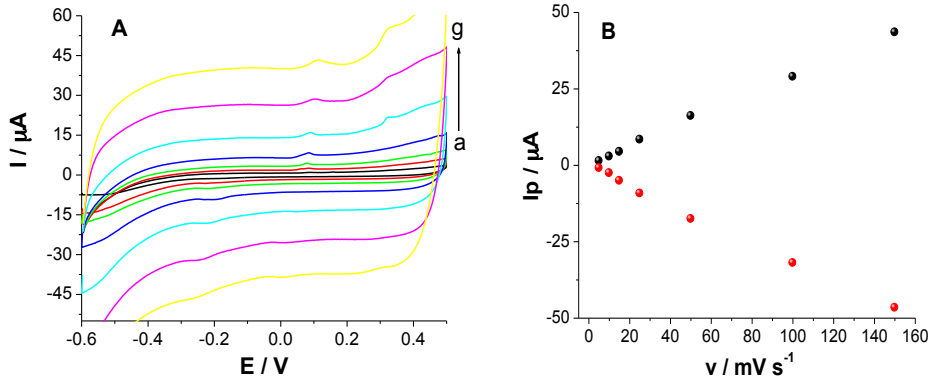

Figure 4.

(A) CVs obtained for 10^{-4} mol/L **A4** solution in ethanol: 0.002 mol/L citrate buffer (pH = 6.5) 1: 4 for different scan rates, from a to g: 5, 10, 25, 50, 100, 150 mV/s. (B) The dependence between the peak current value and the scan rate for the oxidation (black) or reduction peaks (red)

Influence of the scan rate. The influence of the scan rate on the oxidation and reduction potentials ($E_{p,a}$; $E_{p,c}$) and the peak current intensities ($I_{p,a}$; $I_{p,c}$) corresponding to the electrochemical transformation of the **A4** derivative to the GCE surface was investigated. CVs obtained in the range of 0.01 - 0.15 V/s are shown in Figure 4A. The peak current intensity varies linearly with the scan rate (Figure 4B), suggesting that the electrochemical oxidation process of the **A4** derivative at the GCE surface is controlled by adsorption. The variation of the oxidation peak current is correlated with the scan rate following a linear equation:

$$I_{p,a} = 0.288\ v + 0.46,\ (R^2 = 0.998),$$

while the reduction peak current variation is correlated with the scan rate following an equation:

$$I_{p,c} = -0.314\ v - 0.41,\ (R^2 = 0.996),$$

both equations having very good correlation coefficients.

The dependence between $E_{p,a}$ and the logarithm of the scan rate is linear for the domain considered and is characterized by the following equation:

$E_{p,a} = 0.029 \log v + 0.042$, ($R^2 = 0.992$),

while the variation between $E_{p,c}$ and the scan rate logarithm is characterized by the following equation:

$E_{p,c} = -0.06 \log v - 0.013$, ($R^2 = 0.998$),

both equations having very good correlation coefficients.

Influence of the concentration. DPVs on GCE were recorded for solutions with different concentrations of the four compounds, prepared in 0.1 mol/L TRIS buffer (pH = 7.2). The results are shown in Table II.

Thus, for **A1** and **A3**, DPVs were plotted in the oxidation potential range, from 0 to 0.9 V *vs*. Ag/AgCl. An increase in the intensity of the oxidation peak current is observed with the increase of **A1** and **A3** concentration for the range of investigated concentrations (1 µmol/L - 500 µmol/L). For **A2** the DPV were plotted in the reduction potential range, from -0.5 to -0.9 V *vs*. Ag/AgCl.

The values of the detection limits and the linear domain of the studied compounds are presented in Table II.

Table II

Reduction/oxidation currents vs. concentration equations for **A1**, **A2** and **A3**

Compound	$I_p(\mu A) = f(C_{acridina})(\mu M)$	Linear domain (µM)	R^2	Limit of detection (µM)
A1	$I_p = 0.006 \cdot C + 0.994$	1 ÷ 500	0.996	0.33
A2	$I_p = -0.011 \cdot C - 0.953$	1 ÷ 1000	0.991	0.33
A3	$I_p = 0.005 \cdot C + 0.131$	1 ÷ 500	0.994	0.33

A low intensity oxidation signal was obtained for **A4** even at a higher concentration with all investigated electrode materials and supporting electrolytes. Thus, it was observed that there is no correlation between the registered electrochemical signal and the concentration of **A4,** which leads to the impossibility of using this analyte as a DNA intercalating agent for the development of an electrochemical aptasensor. However, by increasing the **A4** concentration, an increase in the fluorescence intensity of this compound was observed in the presence of the dopamine-specific DNA sequence, which would eventually allow the development of a fluorescence sensor.

Determination of interstitial constants between aptamer and A4 derivative

In order to study the interaction between aptamer and **A4** in solution by NMR spectroscopy, two stock solutions were prepared in buffered D_2O/DMSO-d_6 (1:2), the first containing 3.24 µmol/L aptamer and the second 3.24 µmol/L aptamer and 10 mmol/L acridine, respectively. Thus, a set of samples was prepared in which the concentration of aptamer were kept constant at 3.24 µmol/L, while the concentration of **A4** varied between 3 and 10 mmol/L.

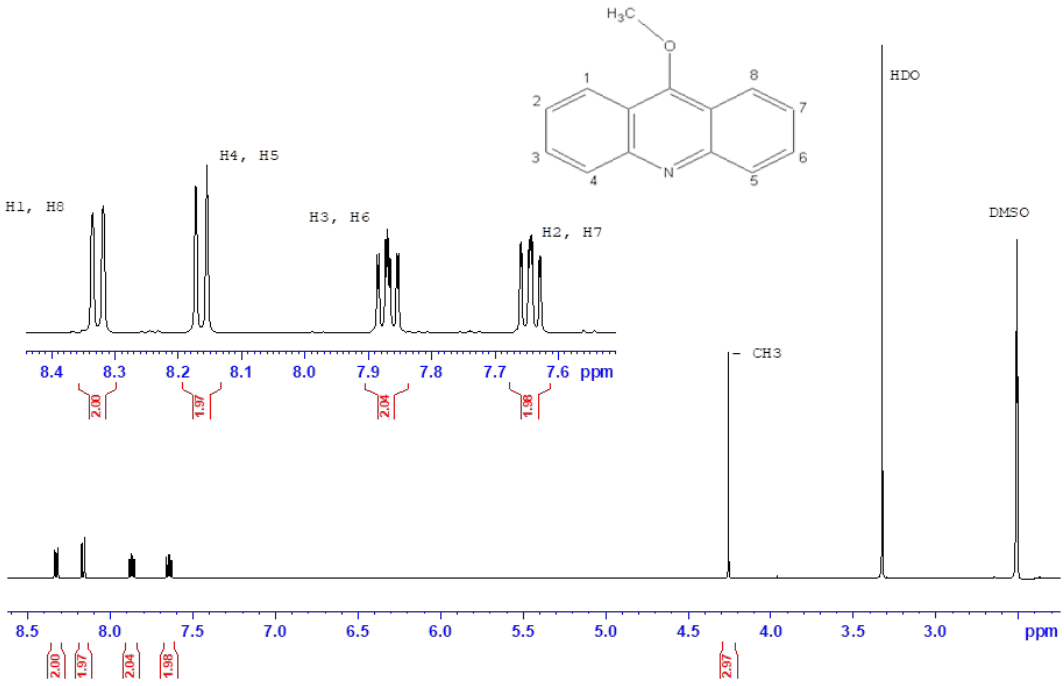

Figure 5.

The ^{1}H-NMR spectrum of **A4** in DMSO-d_6; inset: chemical structure of **A4** (the numbers correspond to proton positions)

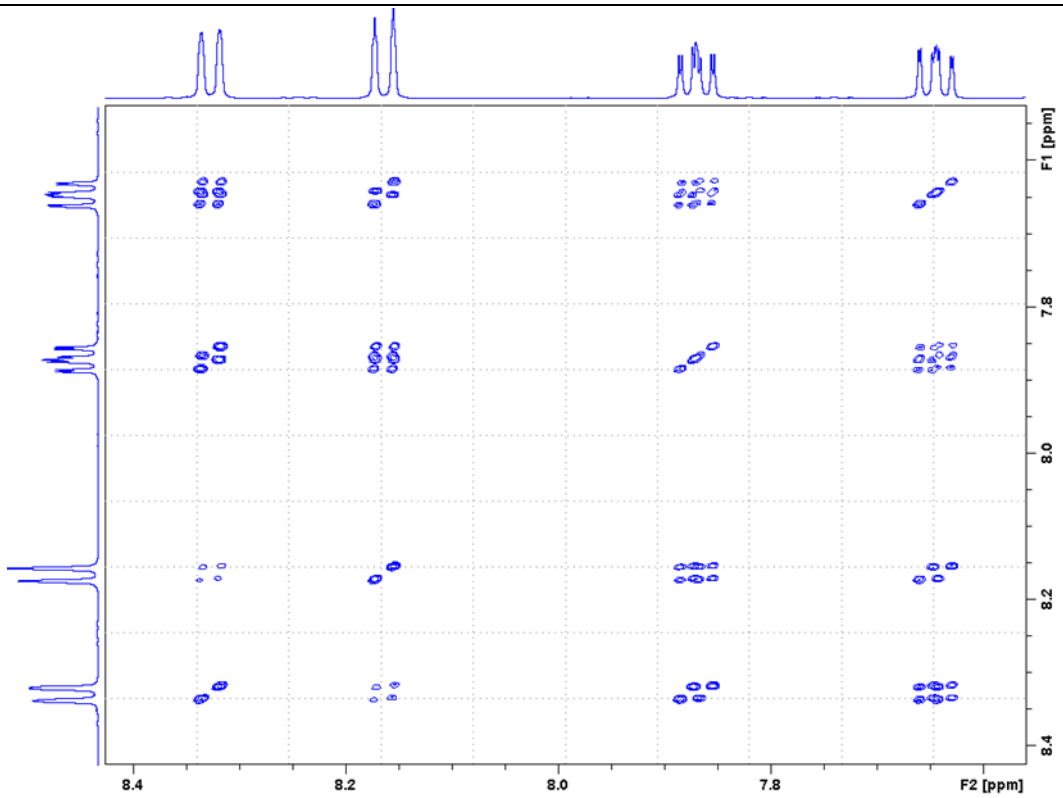

Figure 6.
^{1}H-^{1}H COSY NMR spectrum of **A4**

Figure 5 represents the ^{1}H-NMR spectrum of **A4** with assignment of the signals, considering the numerical order from the inset figure. For a good assignment of ^{1}H-NMR spectrum, the two-dimensional ^{1}H-^{1}H COSY NMR spectrum (Correlation Spectroscopy) of **A4** was considered, which describes the interactions between neighbour protons (Figure 6).

The association constant K_a can be evaluated using NMR, from the observed variation in the chemical shift (differences), spin lattice relaxation time or diffusion coefficient. The interaction between **A4** and aptamer, using the chemical shift variation for H4 and H5 **A4** NMR lines was evaluated.

Ligand binding is analysed using a fast-reversible binding process. The observed chemical shifts of the protons belonging to ligand can be regarded as a weighted average of the free (δ_{free}) and bound (δ_{bound}) forms:

$$\delta_{obs} = f_{free} \cdot \delta_{free} + f_{bound} \cdot \delta_{bound},$$

where $f_{free} = [L]/C_L$ and $f_{bound} = 1 - f_{free}$ represents the molar fractions of the ligand in the free and bound forms, respectively and C_L is the total concentration of the ligand.

The association constant, K_a was evaluated by a linear curve regression analysis of the observed chemical shift changes of the **A4** NMR lines as a function of concentration, according to the following equation [5]:

$$\frac{1}{\Delta\delta_{obs}} = \frac{K_D}{(\delta_{bound} - \delta_{free})[P]_0} + \frac{1}{(\delta_{bound} - \delta_{free})[P]_0}[L]_0$$

where: $\Delta\delta_{obs} = \delta_{free} - \delta_{obs}$; $K_D = ([P][L])/[PL]$; $[L] = [L]_0 - [PL] \approx [L]_0$; $K_D = \{([P]_0 - [PL])[L]_0\}/[PL]$; $K_D = 1/K_a$; P = aptamer; L = ligand (**A4**).

The result obtained after fitting, indicate a weak interaction between H4 and H5 protons of **A4** and aptamer, characterized by an association constant $K_a = 78.43\ M^{-1}$.

Conclusions

The electrochemical and spectral characterization of acridine-*N*-oxide (**A1**) and its derivatives functionalized at position 9 of the acridine nucleus with cyan (9-cyano-acridine-*N*-oxide: **A2**), carboxyl (9-carboxy-acridine-*N*-oxide: **A3**) and methoxy groups (9-methoxy-acridine-*N*-oxide: **A4**), were achieved. The use of these compounds as new DNA intercalating agents for the development of label-free biosensors for biomedical applications was studied. Both the 9-cyano-acridine-*N*-oxide and 9-carboxy-acridine-*N*-oxide derivatives were found to correlate the oxidation or electrochemical electrolysis with slightly acidic pH. For the methoxy derivative of acridine-*N*-oxide it was observed that electrochemical transformation is governed by adsorption at the surface of the electrode, but no correlation could be made between the recorded DPV signal and its concentration. However, an increase in fluorescence intensity of this compound has been

observed with increased concentration in the presence of the dopamine-specific DNA sequence, which opens the possibility of developing a fluorescence apta-sensor for dopamine detection. The association constant of 78.43 M^{-1} based on the results obtained with NMR spectroscopy was calculated.

Acknowledgement

This work was supported by a grant of the Romanian National Authority for Scientific Research and Innovation, CCCDI – UEFISCDI, project number PN-III-P3.1-PM-RO-FR-2016-0003.

References

1. Albert A, The Acridines: Edward Arnold, 1966; 269-271.
2. Bamfield P, Hutchings M, Chromic phenomena: Technological Applications of Colour Chemistry: Cambridge Royal Society of Chemistry, 2010; 7.
3. Cholewiński G, Dzierzbicka K, Kołodziejczyk AM, Natural and synthetic acridines/acridones as anti-tumor agents: their biological activities and methods of synthesis. *Pharmacol Rep.*, 2011; 63: 305-336.
4. Florea A, Ravalli A, Cristea C, Săndulescu R, Marrazza G, An Optimized Bioassay for Mucin1 Detection in Serum Samples. *Electroanal.*, 2015; 27: 1594-1601.
5. He J, Wu D, Zhai Y, Wang Q, Ma X, Yang H, Li H, Interaction of inosine with human serum albumin as determined by NMR relaxation data and fluorescence methodology. *J Molec Liquid*, 2016; 219: 547-553.
6. Jambrec D, Haddad R, Lauks A, Gebala M, Schuhmann W, Kokoschka M, DNA Intercalators for Detection of DNA Hybridisation: SCS(MI)–MP2 Calculations and Electrochemical Impedance Spectroscopy. *Chem Plus Chem.*, 2016; 81: 604-612.
7. Kožurková M, Sabolová D, Janovec L, Mikeš J, Koval' J, Ungvarský J, Stefanisinova M, Fedorocko P, Kristian P, Imrich J, Cytotoxic activity of proflavine diureas: Synthesis, antitumor, evaluation and DNA binding properties of 1′,1″-(acridin-3,6-diyl)-3′,3″-di-alkyldiureas. *Bioorg Med Chem.*, 2008; 16: 3976-3984.
8. Kumar GS, Basu A, A biophysical investigation on the binding of proflavine with human hemoglobin: Insights from spectroscopy, thermodynamics and AFM studies. *J Photochem Photobiol B: Biolog.,* 2016; 165: 42-50.
9. Marian IO, Bonciocat N, Cristea C, Săndulescu R, Bucşa M, Vlassa M, Spectroelectrochemical Study of 9-Substituted Acridines with Potential Antitumor Activity. *Electroanal.*, 2010; 22: 542-548.
10. Mascini M, Palchetti I, Tombelli S, Nucleic acid and peptide aptamers: Fundamentals and bioanalytical aspects. Angew. *Chem Int Ed.*, 2012; 51: 1316-1332.
11. McGhee JD, von Hippel PH, Theoretical aspects of DNA-protein interactions: co-operative and non-co-operative binding of large ligands to a one-dimensional homogeneous lattice. *J Mol Biol.*, 1974; 86: 469-489.
12. Nafisi S, Saboury AA, Keramat N, Neault JF, Tajmir-Riahi HA, Stability and structural features of DNA intercalation with ethidium bromide, acridine orange and methylene blue. *J Mol Struct.*, 2007; 827: 35-43.
13. Rescifina A, Zagni C, Varrica MG, Pistarà V, Corsaro A, Recent advances in small organic molecules as DNA intercalating agents: synthesis, activity, and modeling. *Eur J Med Chem.*, 2014; 74: 95-115.
14. Sassolas A, Blum LJ, Leca-Bouvier BD, Electro-chemical aptasensors. *Electroanal.*, 2009; 21: 1237-1250.
15. Sohrabi N, Binding and UV/Vis spectral investigations of interaction of Ni(ll) piroxicam complex with calf thymus deoxyribonuclei acid (Ct-DNA): a thermodynamic approach. *J Pharm Sci Res.*, 2015; 7: 533-537.
16. Tremiliosi-Filho G, Dall'Antonia LH, Jerkiewicz G, Growth of surface oxides on gold electrodes under well-defined potential, time and temperature conditions. *J Electroanal Chem.*, 2005; 578: 1-8.
17. Vantová Z, Paulíková H, Sabolová D, Kožurková M, Sucháňová M, Janovec L, Kristian P, Imric J, Cytotoxic activity of acridin-3,6-diyl dithiourea hydrochlorides in human leukemia line HL-60 and resistant subline HL-60/ADR. *Int J Biol Macromol.*, 2009; 45: 174-180.
18. Zhang L, Jiang X, Wang E, Dong S, Attachment of gold nanoparticles to glassy carbon electrode and its application for the direct electrochemistry and electrocatalytic behavior of hemoglobin. *Biosens Bioelectron.*, 2005; 21: 337-345.